Journal of Modern Optics, 2013
http://dx.doi.org/10.1080/09500340.2013.803622

Taylor & Francis
Taylor & Francis Group

Spectral responsivity-based calibration of photometer and colorimeter standards

George P. Eppeldauer*

National Institute of Standards and Technology, 100 Bureau Drive, Gaithersburg, MD 20899, USA

(*Received 5 March 2013; final version received 3 May 2013*)

Several new generation transfer- and working-standard illuminance meters and tristimulus colorimeters have been developed at the National Institute of Standards and Technology (NIST) [1] to measure all kinds of light sources with low uncertainty. The spectral and broad-band (illuminance) responsivities of the photometer (Y) channels of two tristimulus meters were determined at both the Spectral Irradiance and Radiance Responsivity Calibrations using Uniform Sources (SIRCUS) facility and the Spectral Comparator Facility (SCF) [2]. The two illuminance responsivities agreed within 0.1% with an overall uncertainty of 0.2% ($k = 2$), which is a factor of two improvement over the present NIST photometric scale. The first detector-based tristimulus color scale [3] was realized. All channels of the reference tristimulus colorimeter were calibrated at the SIRCUS. The other tristimulus meters were calibrated at the SCF and also against the reference meter on the photometry bench in broad-band measurement mode. The agreement between detector- and source-based calibrations was within 3 K when a tungsten lamp-standard was measured at 2856 K and 3100 K [4]. The color–temperature uncertainty of tungsten lamp measurements was 4 K ($k = 2$) between 2300 K and 3200 K, which is a factor of two improvement over the presently used NIST source-based color temperature scale. One colorimeter was extended with an additional (fifth) channel to apply software implemented matrix corrections. With this correction, the spectral mismatch caused color difference errors were decreased by a factor of 20 for single-color LEDs.

Keywords: color calibration; detector-based colorimetry; illuminance responsivity; LED colorimetry; matrix correction; photometer standard; tristimulus colorimeter

1. Introduction

Change of the source standards to detector standards in the photometric and color scale realizations resulted in significant improvements in the scale uncertainties at the National Institute of Standards and Technology (NIST). The NIST detector-based photometric scale [5] was based on the development of a group of eight illuminance meters. They contained the Commission Internationale de l'Eclairage (CIE) standardized $V(\lambda)$ matching filters equipped with temperature monitors and specially selected silicon photodiodes and photocurrent measuring electronic circuits. These photometers still hold the photometric scale with a long-term illuminance responsivity change of less than 0.1%. Working standard photometers with analog temperature control were also developed to disseminate the scale easier.

The illuminance responsivity scales have been realized at two different calibration facilities. The scale, published in 1996, has a relative expanded uncertainty of 0.39% ($k = 2$) [5]. With the development of the Spectral Irradiance and Radiance Responsivity Calibrations with Uniform Sources (SIRCUS) facility [6], the spectral irradiance responsivity uncertainty could be lowered compared to the Spectral Comparator Facility (SCF) based scale [5]. It was studied how to improve the uncertainty of the SCF based scale. In order to satisfy this goal, high quality transfer standard photometers have been developed. These transfer standards can be calibrated not only at the SCF, but also at the SIRCUS. At SIRCUS, stabilized tunable-lasers are coupled into integrating sphere sources producing uniform irradiance for the irradiance measuring Si trap detectors and the illuminance measuring photometers. As a result of the SIRCUS used calibration geometry, the uncertainty of the SIRCUS made spectral irradiance responsivity calibrations can be dominated by the 0.06% ($k = 2$) uncertainty of the Si trap-detector [6]. However, the photometer standards, developed for the SCF-based scale realization [5], cannot be calibrated at the SIRCUS because the remaining coherence at the sphere outputs can cause large interference fringes. Development of improved transfer standards was needed to fix this problem. The SCF-based calibration had a longer scale derivation chain than the SIRCUS-based calibration since the transfer standard photometers were calibrated against the photometer standards used in the SCF-based scale realization. The substitution method was applied when both photometers measured the same illuminance of a 2856 K lamp. The

*Email: george.eppeldauer@nist.gov

difference of the SIRCUS and SCF determined illuminance responsivity measurements was 0.4% [1]. Though, this difference is within the reported uncertainties of the two different scale realizations of the two facilities, the goal was to decrease this difference and to obtain a better agreement between the two scales. In order to achieve this goal, the major uncertainty components of the two independent photometric scale realizations were analyzed, improved, and then compared.

The introduction of the spectral responsivity based calibration of tristimulus colorimeters [3] made it possible to measure the color of light sources fast and with low uncertainty. The color-measurement uncertainty can be low only if the spectral responsivities of the colorimeter channels are measured with low uncertainty. To achieve this goal, new tristimulus colorimeters were developed where the spectral responsivity calibration of the channels can be performed with an uncertainty of 0.15% (k = 2). This responsivity-uncertainty resulted in an expanded uncertainty of 4 K (k = 2) in color temperature measurements of tungsten lamps [4]. The low-uncertainty responsivity calibrations in certain wavelength intervals of several special light source distributions (such as blue or red LEDs) still could not result in low color measurement uncertainties because the spectral match of the realized colorimeter-channels to the CIE color matching functions was poor and could not be improved. A solution to this problem was to extend the detector-based calibration method of tristimulus colorimeters with an alternative matrix correction procedure [7] that can decrease the spectral mismatch error for specific types of light sources such as LEDs.

The main design issues and characteristics of the photometers and tristimulus colorimeters, the spectral responsivity calibrations, the illuminance responsivity and color temperature scale-realizations and scale-validations, the related measurement issues, and the improvements obtained with the matrix corrections are discussed here when different kinds of light sources are measured.

2. Photometer transfer standards

The transfer standards were designed such that it is the uncertainty of the spectral irradiance responsivity calibrations that determines the photometric scale uncertainty and not limitations in the performance of the photometers themselves. New filter combinations have been designed with a minimum allowed thickness of 4.5 mm to avoid interference fringes. They are individually fabricated to closely match the responsivity of the silicon detector to the CIE $V(\lambda)$ function [8]. The filter combinations are in a filter wheel located between the common detector and aperture. The wheel temperature is controlled at 25 °C where the spectral mismatch errors were minimized. Two types of transfer standard photometers were designed and built. The first type, as shown in Figure 1, uses windowless silicon photodiodes in a tunnel trap configuration [9]. The cut-outs were made for better illustration. A temperature controlled filter-wheel was inserted and moved between the input aperture and the silicon tunnel-trap detector. The long-term stability of this photometer was regularly monitored to see if any responsivity changes happen due to either stain settlement on the filter surfaces or because the photodiodes are exposed to the ambient air. The stain from the front of the filter combinations was removed yearly using isopropyl alcohol. Still, the illuminance responsivity decreased with 0.2% from 2003 to 2007 and with another 0.1%–0.15% to 2009. The change was close to 0.5% at 400 nm and it gradually decreased and became negligibly small at 500 nm. In this tunnel-trap detector, light is not reflected back to the filters.

In the improved (newer) transfer standard, a single-element silicon photodiode is used which has a sealed wedged-window to avoid fringes. The picture of this transfer standard (with the front panels removed) is shown in Figure 2. The front panels are removed for

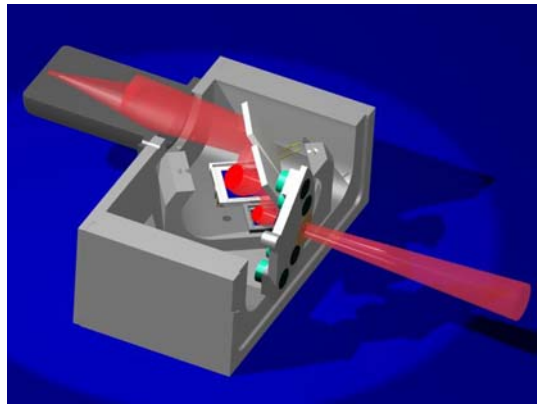

Figure 1. The filter-trap transfer standard.

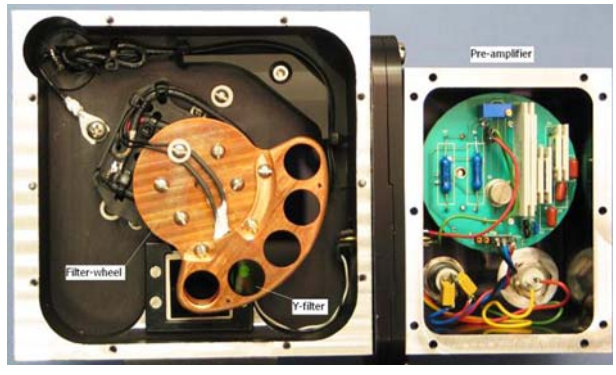

Figure 2. The new generation transfer standard.

better illustration. The photo shows the light tight box with the detector and the filter-wheel inside. The Y-channel is used as an absolute photometer. The photocurrent meter is attached to the side of the box. The current measuring electronics are matched to the electronic characteristics of the photodiode for low-noise performance. A signal dynamic range of 12 decades was achieved. The uncertainty of the current-to-voltage conversion is less than 0.02% ($k = 2$).

The detector is a large-area (1 cm × 1 cm) single-element silicon photodiode. The 0.5° wedge of the sealing window was needed to avoid interference fringes in the output signal of the photodiode. The spaces on the two sides of the temperature controlled filter-wheel are small resulting in five orders of magnitude blocking in the IR even in overfilled mode. The less than 0.3% peak-to-peak fringes of the Y-channel (as measured at the SIRCUS) before (solid line) and after filtering (smoothing) the data are shown in Figure 3. The filter-plus-detector combination was individually optimized to the CIE standard $V(\lambda)$ function. No responsivity degradation could be measured on this improved photometer between 2007 and 2009.

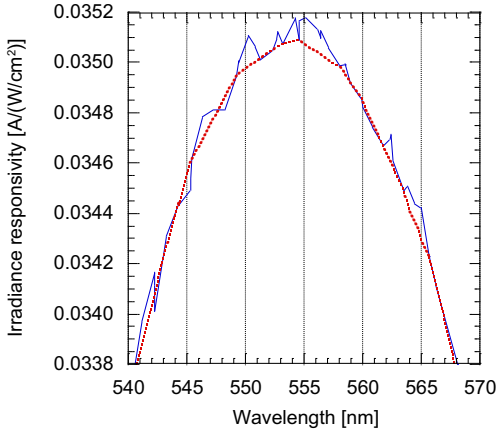

Figure 3. Filtered fringes of the SIRCUS measured trap photometer. (The color version of this figure is included in the online version of the journal.)

Also, the baffling inside of the trap-detector used photometer was not efficient enough. Figure 4 shows that in overfilled mode (at SIRCUS), because of the internal reflections of the photometer, the Si trap detector (that peaks at 970 nm), measured a small portion of the incident light which did not go through the $V(\lambda)$ filter. In under-filled mode (at SCF), the stray and reflected light attenuation was two orders of magnitude better.

3. Photometer working standards

The illuminance responsivities of the presently used working standard photometers (used in the SCF-based scale realization) have been determined yearly based on their spectral power responsivity measurements at the SCF. Figure 5 shows the long-term changes normalized to unity in 1991. Yearly scale realizations were made to determine the actual responsivities based on the SCF scale realizations. The thick line shows a 0.3% maximum responsivity change for the group-average of photometers 4, 6, and 8. The front surfaces of the filters

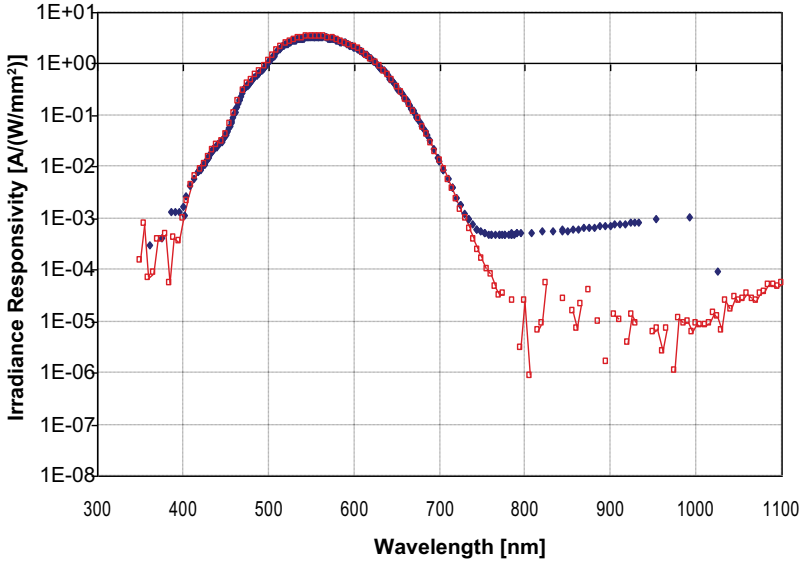

Figure 4. SIRCUS (full diamonds) and SCF (open squares) measured trap photometer irradiance responsivities, including the unfiltered internal stray and reflected light. (The color version of this figure is included in the online version of the journal.)

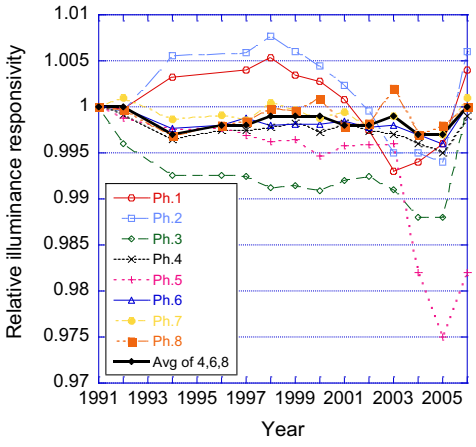

Figure 5. Long-term changes of the photometer standards used in the SCF-based scale realization. All photometers were cleaned in 2006 and Ph.1 and Ph.2 were cleaned first in 1994. Ph.5 is an outlier, rejected from the group. (The color version of this figure is included in the online version of the journal.)

in photometers 1 and 2 were cleaned first in 1994. The other photometers were not cleaned until 2006, when the front surfaces of all photometer filters were cleaned using isopropyl alcohol and a lens cleaning tissue. The results show that the long term stability of the individual photometers can be improved to ±0.1% if the front surfaces of the filters are cleaned on a regular basis. Photometer 5 was damaged, repaired, and rejected from the group.

Ten-year long changes of 0.02% were reported on silicon photodiodes sealed with fused silica windows [10] used in these working standards. It can be concluded that change-free photometer standards can be made if the photometer head is sealed with a fused silica window. The stability of the working standards should be matched to the lower uncertainty of the SIRCUS-based scale to obtain an overall uncertainty improvement in the disseminated scale. A package design was applied for all photometers to obtain a uniform temperature distribution for the filter combination and the silicon photodiode. The cut-on edges of the glass filter layers (in the filter combination) that determine the steep short-wavelength slope of the $V(\lambda)$ curve are temperature dependent. Also, the applied infrared-suppressed silicon photodiode has a significant temperature coefficient of responsivity at wavelengths longer than 630 nm. These two components are mounted in a metal housing, and the uniform temperature is monitored in the photometers used in the SCF-based scale realization [5], and stabilized in the new (second generation) working standards. As shown in Figure 6, the aperture (blue), the filter combination (green), and the photodiode (brown) are close to each other inside of a Copper pot (black). While there is a small gap between the photodiode and the filter, the very thin aperture is mounted on the front surface of the

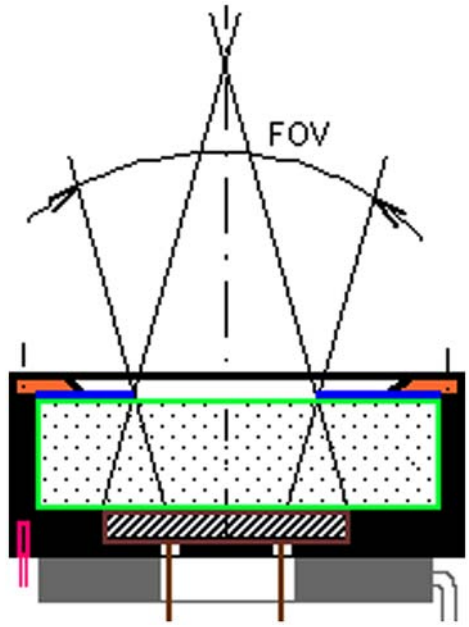

Figure 6. Structure of a photometer package. The unvignetted FOV is shown. (The color version of this figure is included in the online version of the journal.)

filter to avoid inter-reflections. In order to simplify cleaning the front surface of the filter, the aperture is fixed in a holder (orange) that can be easily removed and relocated into the same position using an asymmetric screw arrangement. A temperature sensor (pink) is plugged into the copper pot. A ring shape thermoelectric cooler (gray) is mounted to the bottom of the copper pot in the new (second generation) working standards to keep the temperature constant, just above the ambient.

The field-of-view (FOV) of the illuminance meter depends on the diameter of the aperture and the photodiode active area. It is always kept small (in this case, the shown unvignetted FOV is 11°) to reject ambient light as well as reflections and stray light from a test light-source. The base unit, as shown on the right side of Figure 7, can be equipped with a bayonet mount at the front to attach an input optic for luminance measurement. In this example, the filter can be removed therefore its temperature is independently controlled from the temperature of the photodiode. The photocurrent meter is located inside of another cylindrical housing attached to the bottom of the base unit (on the right side). The electronic characteristics of the current-to-voltage converter are matched to the high shunt resistance of the silicon photodiode to obtain low output-noise and wide signal range.

4. Photometer responsivities

While the SIRCUS facility can measure irradiance, the basic operational mode of the SCF facility is radiant power measurement. It was necessary to determine the

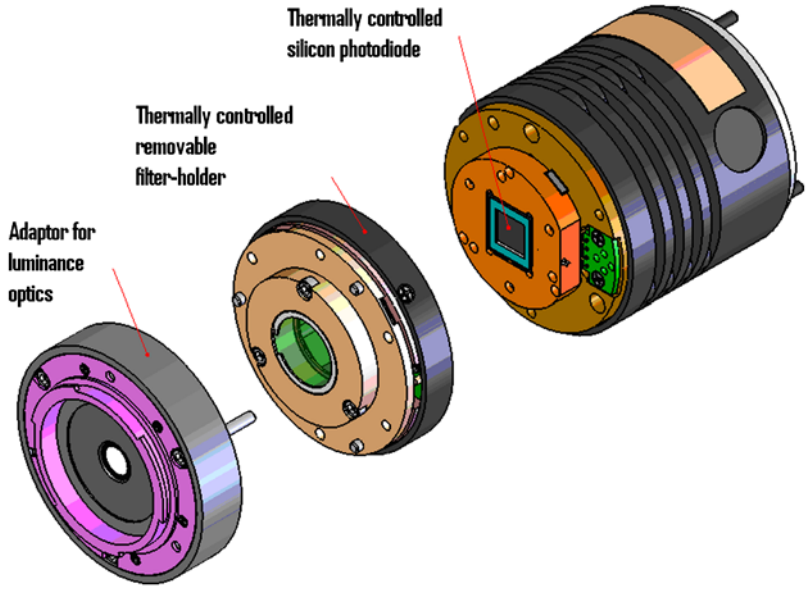

Figure 7. A new (second) generation photometer working standard. (The color version of this figure is included in the online version of the journal.)

aperture areas for both types of transfer standard photometers. The aperture areas were determined from a raster-scan method at the SCF when the photopic filter was removed from the photodiode. The f/9 scanning beam did not cause multiple reflections between the aperture and the detector because of the 14 mm separation between them in the new transfer standard photometers. The aperture areas were also determined from an irradiance-to-power responsivity ratio measurement at the SIRCUS. In this case, the irradiance responsivity was performed with a 'point source' geometry and the area determination was made against the known aperture area of a Si-trap detector of the SIRCUS (at one laser wavelength). The trap-detector aperture was calibrated at the NIST aperture-area calibration facility with 0.02% (k = 2) uncertainty [11]. The obtained aperture areas are shown in Table 1.

The difference between the SIRCUS and the SCF measured areas was 0.11%. The relative expanded uncertainties of both methods were less than 0.08% (k = 2).

The 5 mm diameter aperture of the transfer standard photometers caused a beam clipping during the spectral power responsivity calibrations at the SCF. The 1.1 mm diameter monochromatic beam imaged to the aperture plane had some spatially scattered light (halo) around the aperture-hole which was clipped by the aperture itself. The halo was caused by imaging problems. Because of the clipping, less flux was measured by the photometers than with the reference Si detector of the SCF. The loss caused by the beam clipping was measured using a 10 mm diameter silicon photodiode and a 5 mm diameter aperture (from the same batch as the photometer aperture). The aperture was in front of the detector during one spectral scan and then removed for the second measurement. The max-min change of the spatial non-uniformity of the silicon photodiode was within 0.1% inside of the illuminated area. Figure 8 shows the per-cent response difference obtained from the two measurements.

Table 1. Measured aperture areas of the transfer-standard photometer (F100) built with a single-element Si photodiode.

	SIRCUS	SCF
Area (mm^2)	19.730	19.708

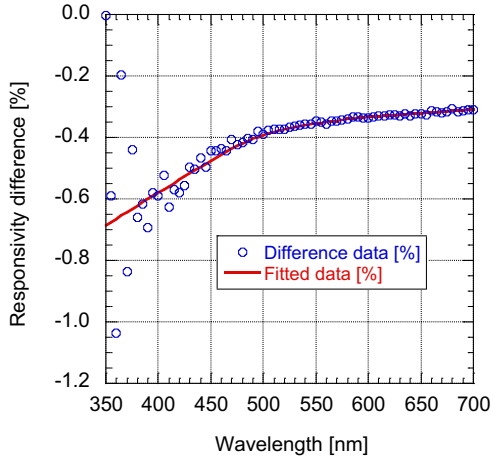

Figure 8. Response difference of two SCF responsivity measurements made with and without a 5 mm aperture in front of a large Si photodiode. (The color version of this figure is included in the online version of the journal.)

The beam clipping was wavelength dependent. To decrease this dominating uncertainty component of the spectral power responsivity calibration, a wavelength dependent correction was applied to the photometer spectral responsivity data. As a result of this correction, the 0.3% to 0.6% systematic errors decreased to 0.05% for the overall visible range.

The measured aperture area was multiplied by the SCF measured spectral power responsivity of the photometer to obtain the SCF-based spectral irradiance responsivity. During the SCF calibrations, the wavelength shift of the monochromator was minimized to less than 0.1 nm before the spectral responsivity scans.

The SIRCUS and SCF measured spectral irradiance responsivities of the transfer-standard photometer built with a single-element Si photodiode (F100) are shown in Figure 9. The logarithmic scale shows that equal blocking was measured in both power and irradiance measurement modes.

The SCF-based spectral irradiance responsivity of both transfer standard photometers was compared to the SIRCUS measured spectral irradiance responsivity. The absolute difference for the trap-detector based photometer is shown in Figure 10. The graph also shows the SCF determined spectral irradiance responsivity around the peak responsivity of the trap-photometer. The structures in the difference curve are caused by the filtered fringes of the SIRCUS data.

The spatial uniformity of responsivity of the F100 photometer is shown in Figure 11. The spatial scan was made at 555 nm with 0.5 mm increments. The diameter of the scanning spot was 1.1 mm. The 0.1% contours

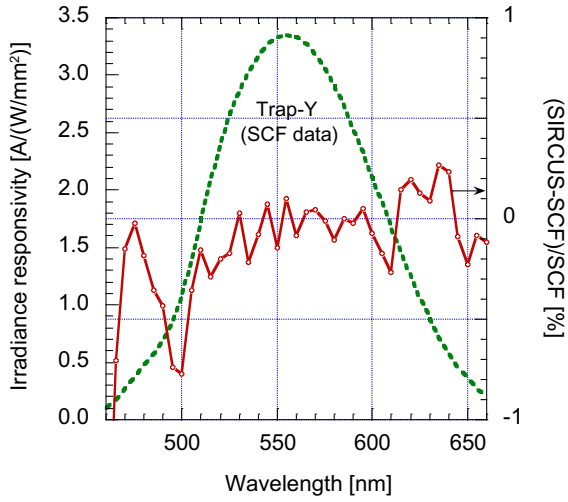

Figure 10. Difference of the SIRCUS and SCF measured spectral irradiance responsivities of the trap photometer. (The color version of this figure is included in the online version of the journal.)

illustrate the combined spatial non-uniformity of the illuminance measuring photometer including the transmittance changes of the photopic filter combination and the responsivity changes of the Si photodiode.

The current-to-voltage converters of the transfer standard photometers were calibrated against the new NIST reference current-to-voltage converter which has an uncertainty of 0.013% (k = 2) for all gain selections up to 10^{10} V/A [12]. This uncertainty is about six times smaller than the present amplifier-gain calibration uncertainty at the SCF.

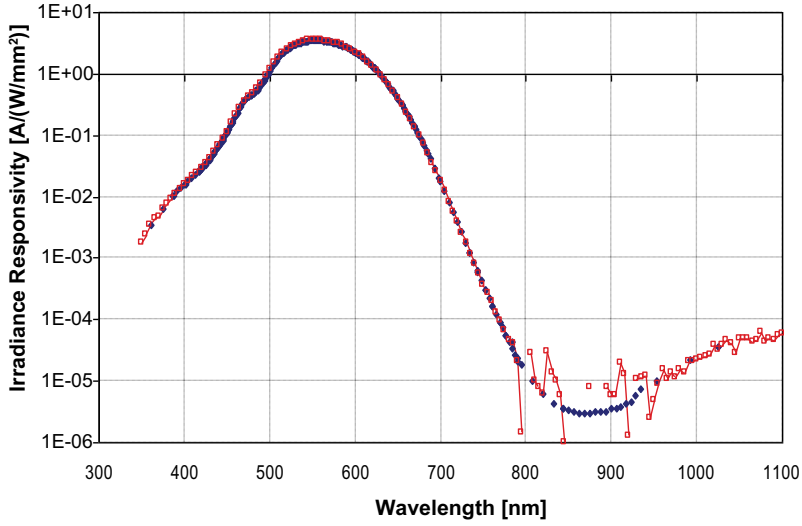

Figure 9. SIRCUS (full diamond) and SCF (open square) measured spectral irradiance responsivities of the F100 photometer. (The color version of this figure is included in the online version of the journal.)

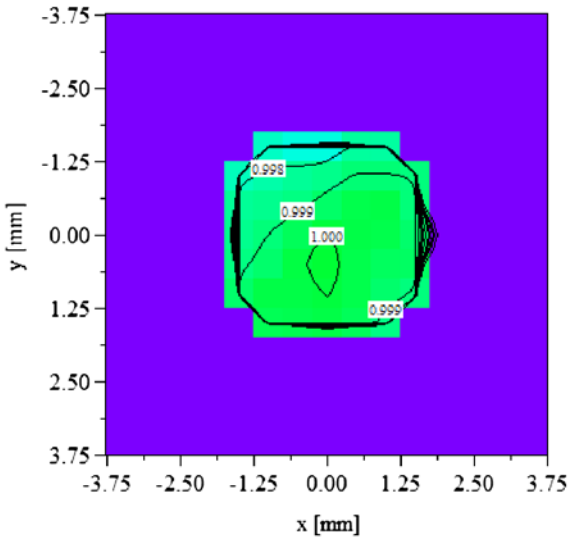

Figure 11. Spatial non-uniformity of responsivity of the F-100 photometer. (The color version of this figure is included in the online version of the journal.)

4.1. Illuminance responsivities

The illuminance responsivity, s, which is the ratio of the photometer output current to the illuminance measured by the photometer, was determined from the SIRCUS measured spectral irradiance responsivity $s_E(\lambda)$ and the incident irradiance $E(\lambda)$ from a CIE Standard Illuminant A source:

$$s = \frac{\int s_E(\lambda)E(\lambda)d\lambda}{K_m \int V(\lambda)E(\lambda)d\lambda},$$

where K_m is the maximum spectral luminous efficacy, 683 lm/W, and λ is the wavelength.

After the spectral irradiance responsivity comparisons, the illuminance responsivities of the transfer standard photometers were calculated [8]. Though the $V(\lambda)$ function is defined only from 360 nm to 830 nm, the integral of both the numerator and the denominator was extended for the 350 nm to 1300 nm range to minimize errors from filter leakage and fluorescence. The illuminance responsivity comparison (directly calculated from the SCF and SIRCUS spectral irradiance responsivities) for the trap and F-100 transfer standard photometers is shown in Table 2.

The 2007 (first) lines for both photometers show an indirect comparison of the illuminance responsivities. In the indirect comparison, the SCF-based illuminance responsivity was not directly derived from the SCF measured spectral responsivity. Instead it was transferred from the photometer standards used in the SCF-based scale realization to the transfer standard photometers (that are test devices in this case) using the detector substitution method at the photometer bench. During the substitution, all photometers measured the same 2856 K luminous intensity lamp. The obtained SCF-based illuminance responsivity of the transfer standard photometer was then compared to the SIRCUS-based (directly derived) illuminance responsivity. The 2009 (second) lines show direct comparisons, where not only the SIRCUS but also the SCF-based illuminance responsivities were obtained directly from the spectral irradiance responsivity data. In the F-100 data, the 0.41% deviation between the SIRCUS and the SCF results in 2007 decreased to 0.02% because the uncertainty of the 2009 direct comparison is lower than that of the indirect comparison (using the long SCF plus Photometer Bench derived chain) in 2007. On the F-100, the SIRCUS-based responsivity decreased by 0.2% and the SCF-based responsivity increased by 0.19% between 2007 and 2009. These changes, measured on the stable F-100 photometer, are within the 0.2% (k = 2) combined uncertainty of the SIRCUS and SCF based illuminance responsivity calibrations. This 0.2% (k = 2) uncertainty of the two independent scale realizations is about a factor of two improvement over the existing SCF-based illuminance responsivity scale [5].

Table 2. The illuminance responsivities of the two transfer standard photometers determined at two responsivity calibration facilities.

	SIRCUS		SCF		SIRCUS/SCF
	nA/lx	Year	nA/lx	Year	Ratio
Trap	4.901	2007	4.885	2007	1.0033
Ph.	4.885	2009	4.887	2009	0.9996
F-100	5.187	2007	5.166	2007	1.0041
Ph.	5.177	2009	5.178	2009	0.9998

The decrease obtained in the SIRCUS-based illuminance responsivity of the trap photometer was 0.33% between 2007 and 2009. This change includes a 0.1%–0.15% degradation in the illuminance responsivity of the trap photometer (which decreased another 0.2% from 2003 to 2007). A 0.04% illuminance responsivity difference was measured at the SCF for the trap photometer between 2007 and 2009. This difference also includes the 0.1%–0.15% permanent responsivity degradation of the trap photometer. The 2009 (second) lines in the last column of Table 2 show that the directly determined SIRCUS and SCF illuminance responsivities agree within 0.04% for both reference photometers.

5. Tristimulus colorimeters

Two generations of tristimulus colorimeters have been developed at NIST. The first colorimeter, as shown in Figure 1, was based on a silicon tunnel-trap detector

[1,9,13]. The advantage of this design was that the trap detector can be calibrated for spectral responsivity without receiving any back reflection from the trap-detector. Unfortunately, the trap detectors use windowless photodiodes that are exposed to the ambient air. Because of this problem, a 0.2% decrease was measured in the luminous responsivity of the Y-channel of the trap-colorimeter during four years. Also, there was a roughly 0.1% leakage of the incident light around the filters because the baffling at the input of the trap detector was not efficient enough. In order to eliminate these problems, a second generation tristimulus colorimeter was developed where a single-element Si photodiode with a sealing wedge-window was applied [1]. The picture of this colorimeter is shown in Figure 2. The temperature-controlled copper filter-wheel with five selectable positions is located between the photodiode and the input aperture. The rotating knob (on the back) rotates together with the wheel. The soldering points of the thermoelectric cooler (located on the back side of the wheel) and the thermistor (fixed with low out-gassing epoxy) are strain relieved using a special wire guiding system to avoid breaking because of frequent changes of the filter positions. The preamplifier on the right side of the picture has seven switch-selectable (from the back) gains and a signal dynamic range of 12 decades.

Seven second-generation tristimulus colorimeters were built. The filter combinations of four of these colorimeters were taken from one batch (#1) of the realized filter combinations. The filter combinations of the other three colorimeters were taken from another batch (#2). In both batches, the filter–detector combinations were individually matched to the CIE color matching functions. Figure 12, as an example, shows the realized spectral responsivities of the Y, X1, and Z channels where the filter combinations were taken from batch #1. The peak-normalized X1 (at 595 nm) and Z (at 445 nm) curves show that the relative spectral responses within a group (for both the X1 group and the Z group) are very similar to each other. The Y curves are absolute spectral responsivities of the four colorimeters. The absolute peak responsivities of the 100, 101, and 103 colorimeters are equal within 0.3% but 102 has a 0.7% higher responsivity than the average of the other three. However, when the four relative Y spectral responses are normalized, they are again very similar to each other. Since the relative spectral responsivity curves of all the four colorimeters, for each channel, are very similar, it was possible to calibrate the three working standard colorimeters (101, 102, and 103) against the reference colorimeter 100.

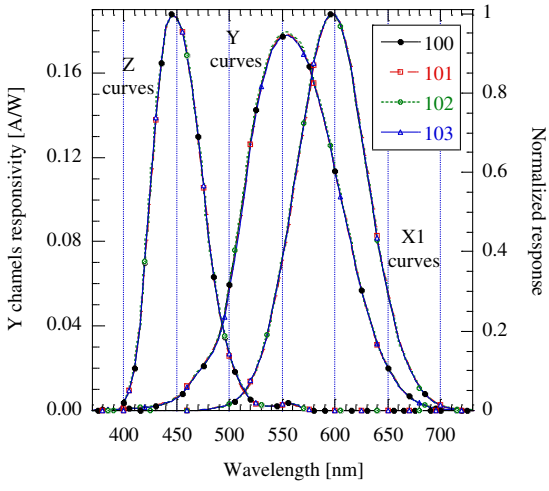

Figure 12. The absolute spectral responsivities of the Y and the normalized spectral responses of the X1 and Z channels of the colorimeters 100, 101, 102, and 103. (The color version of this figure is included in the online version of the journal.)

6. Characteristics of the tristimulus meters

Several cut-on filter components in the X2, Z, and Y filter combinations had small fluorescence and produced spectral responsivity changes. The responsivity curve in the UV region was measured higher than what the transmittance of the filters indicated. The responsivity increase in the UV was minimized by selecting the filter components for low fluorescence, choosing the right order of the filter-layers within a package, and choosing the orientation of the filter-package such that the smallest increase in the responsivity is obtained [13]. Figure 13 illustrates that the responsivity blocking (that includes the blocking of the fluorescence-causing responsivity increase) at 350 nm is more than three orders of magnitude.

When the first four colorimeters (of the seven) were made, the X_2 and Z (blue) filters had significant leakage (increased transmittance) in the near-infrared.

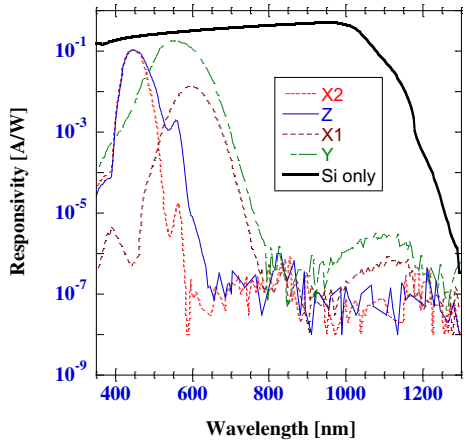

Figure 13. Channel spectral responsivities (in log scale) of the second generation (prototype) colorimeter. (The color version of this figure is included in the online version of the journal.)

Accordingly, the blocking of the X_2 and Z channels was not effective between 700 nm and 1300 nm. The filter combinations of these channels were redesigned and the infrared leakage was decreased to a four orders of magnitude lower level than the peak responsivity of the channels (as seen in Figure 13).

The aperture diameter was 5 mm and the active area of the photodiodes was 18 × 18 mm in the first four colorimeters. The large FOV of the colorimeters (roughly 30° unvignetted FOV and about 80° full FOV) caused sensitivity to stray light in wide angle from the inside wall of the photometer bench, which required careful baffling and masking to minimize effect of the stray light from the test lamps. The active size of the photodiode was decreased to 1 cm^2 to obtain about a factor of two decrease in FOV in the last three colorimeters.

7. Responsivities of the tristimulus meters

The four channels of each colorimeter were calibrated for spectral responsivity. One of the seven second-generation colorimeters was used as a reference colorimeter. Only this colorimeter was calibrated against two reference Si-trap detectors [9] at the SIRCUS [6] facility. Integrating sphere sources with stabilized tunable lasers were used at this facility to determine the absolute spectral irradiance responsivity of the colorimeter channels. Typically, the relative expanded uncertainty of spectral irradiance responsivity calibrations at SIRCUS is 0.1% (k = 2) in the visible region.

The seven, second generation colorimeters including the reference colorimeter were calibrated at the monochromator-based SCF [14]. Here, the spectral power responsivity of the channels was measured with a relative expanded uncertainty of 0.2% (k = 2). The measurements were made against a group of single-element Si working-standard detectors that were calibrated against SIRCUS calibrated Si-trap detectors. In order to determine the spectral irradiance responsivity from the SCF power-responsivity results, the aperture areas were determined from the ratio of the colorimeter irradiance responsivity to its power responsivity at one wavelength. These area determinations were made at the SIRCUS facility using the empty position (no filter) of the filter wheel in a colorimeter. The reference device was a Si tunnel-trap detector with an aperture of known area. The colorimeter's aperture-area times its spectral power responsivity resulted in the spectral irradiance responsivity. The uncertainty of the area determination was 0.11% (k = 2).

The spectral power responsivity of the five channels (including the empty channel where the detector was measured) of one (the reference) of the seven colorimeters is shown in Figure 13. These measurements were made at the SCF to 1300 nm, within the response range of the applied Si-detector, using both Si and InGaAs working standards at the SCF responsivity measurements.

The difference of the channel calibration factors of the reference colorimeter between the SIRCUS and SCF made determinations was 0.11% for the X1 channel and 0.024% for the Y channel. However, the calibration-factor (see below) difference was 0.31% for the Z channel and 0.36% for the X2 channel. One reason that the differences are higher for these blue channels is that the uncertainties of the aperture-clipping caused responsivity corrections at the SCF increased at 400 nm. The uncertainties are about half the magnitude at 500 nm. The aperture correction was needed because the SCF output beam was clipped by the 5 mm diameter apertures of the colorimeters. The beam halo in the output beam of the SCF was produced by the reflectance degradation of the imaging mirrors. The curve shown in Figure 8 was used again for spectral-responsivity correction of the SCF responsivity data. The reason of the data-spread between 400 nm and 500 nm is the poor signal-to-noise ratio. The noise of the measured data increases with decreasing wavelength. The uncertainty of the responsivity correction at 400 nm (caused by the ∼30% spread here) is 15% which corresponds to a responsivity uncertainty of 0.1% (error of the error) at 400 nm.

For validation of the SIRCUS measured spectral responsivities, the differences between the SIRCUS and the SCF determined spectral irradiance responsivities of the blue channels were checked. Figure 14 shows the differences for the X2 and Z channels. The (absolute) differences around the 445 nm peak are within ±0.2%. This point is an outlier since the differences are only 0.2% at 435 nm and 455 nm. Structures like in these dif-

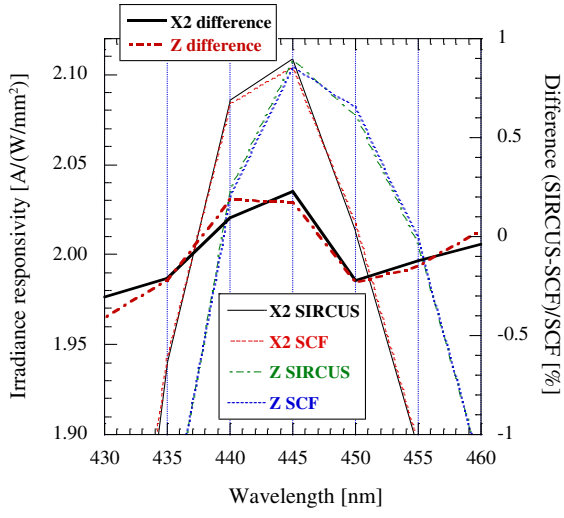

Figure 14. Difference between the SIRCUS and SCF measured spectral irradiance responsivities for the blue channels of the reference colorimeter. (The color version of this figure is included in the online version of the journal.)

ference curves can be seen in all the spectral difference curves of the four channels. The structures are caused by the interference fringes and the interpolation errors in the SIRCUS measured data and also by bandpass errors of the SCF monochromator. The SCF monochromator has a finite bandpass of 4 nm and the data were taken with 5 nm increments. The interpolation of the SIRCUS data was needed to obtain also 5 nm increments from the data taken with different wavelength separations. Another contribution to the responsivity difference comes from the 0.11% (k = 2) uncertainty of the aperture-area measurement of the colorimeter.

The spectral responsivity differences of the blue channels from the SIRCUS and SCF calibrations showed that the spectral responsivities are within an uncertainty of 0.2% (k = 2). Since the working standard colorimeters were calibrated against the SIRCUS calibrated reference-colorimeter (#100) in broad-band mode [13], it was enough to validate that the SIRCUS responsivity uncertainty is less than 0.15% (k = 2). This is the highest allowed responsivity uncertainty to obtain 4 K (k = 2) uncertainty in the color temperature measurements of tungsten lamps [3]. These uncertainties could be somewhat decreased by applying 'filtering' for the interference fringes, which caused structures (bumps) for the SIRCUS measured data around the peak responsivity of the channels.

Also, monochromator bandpass corrections could be applied to further decrease the spectral responsivity errors caused by the 4 nm bandpass. The wavelength increments at the monochromator measurements could be also decreased especially for the blue channels where the bandwidths are smaller and the side-slopes are steeper than for the other two channels.

8. Broad-band (integrated) responsivities and calibration of the tristimulus meters

The channel calibration factors include both the amplitude and the spectral mismatch corrections of the realized channels for broad-band measurements of light sources. Since the Y-channel is used for (absolute) illuminance measurements, the constants in the other three calibration factors are equal to the constant used in this channel. The calibration factor of the Y-channel is the ratio of the CIE tristimulus value to the measured output signal (current) of the Y-channel [1]:

$$k_Y = \frac{Y}{I_Y} = \frac{K_m \int_\lambda E(\lambda) V(\lambda) d\lambda}{\int_\lambda E(\lambda) s_Y(\lambda) d\lambda}$$

where $E(\lambda)$ is the relative spectral distribution of the reference source (which is not a standard in this detector-based calibration), $V(\lambda)$ is the CIE standard photometric observer, and it is also one of the color matching functions of the CIE standard colorimetric observer, K_m is the maximum spectral luminous efficacy, 683 lm/W (used to convert the measured radiometric quantity to photometric quantity), $s_Y(\lambda)$ is the measured spectral irradiance responsivity of the realized channel (calculated from Y) in A/(W/m^2), and λ is the wavelength. Since the illuminance (in lx) is the ratio of the luminous flux (in lm) to the aperture area of the colorimeter (in m^2), the calibration factor of the Y-channel will be obtained in lx/A, which is the reciprocal of the integral responsivity. The integrals were made from 360 nm to 1300 nm (beyond the 830 nm long-wavelength end of the $V(\lambda)$ definition) to perform accurate spectral mismatch corrections when calculating the broad-band calibration factors of the colorimeter channels. The k_{X1}, k_{X2}, and k_Z calibration factors for the other three channels were calculated similarly. The tristimulus values of a test source can be obtained when multiplying the test source produced output current with the calibration factor for all of the four channels [13].

From the tristimulus values the color temperatures are calculated using iterations. First, the u′,v′ chromaticity coordinates are calculated for a range of blackbody temperatures from 1000 K to 20,000 K. From the chromaticity coordinates of the test source, the distance is calculated to the blackbody curve (coordinates). The closest distance is chosen along with its neighbors. In a second step, the set of blackbody temperatures are extended to 20 points centered on the previous closest point and bounded by the neighbors. Again, the smallest distance is chosen along with its neighbors. This process is repeated four more times. The last step will calculate the correlated color temperature to within 0.01 K of the F-100 measured chromaticity coordinate.

9. Validation and recalibration of the tristimulus colorimeters

The working standard tristimulus colorimeters, after calibration against the reference colorimeter in broad-band mode [13], were validated by measuring the color-temperature of a lamp standard. The detector-based color–temperature was calculated from the reference colorimeter measured tristimulus values. The lamp standard was calibrated against blackbody standards (source-based color temperature calibration) at the Facility for Automated Spectral Calibrations (FASCAL) [15]. This validation was performed on the NIST Photometry Bench [5] at different lamp temperatures. As an example, Table 3 shows the results of the source-based (FASCAL determined) and the detector-based (average of colorimeters 101 and 103) calibrations when the F595 lamp standard was measured at two different temperatures.

Table 3. Comparison of source-based and detector-based color–temperature measurements.

Lamp standard	Source-based (from FASCAL)	Detector-based (average of colorimeters 101 and 103)
F595	2856 K	2853.5 K
F595	3100 K	3097 K

During the yearly recalibrations, the working standard (test) colorimeters will be compared to the reference colorimeter(s) (calibrated at the SIRCUS) by measuring a tungsten lamp of about 2856 K color temperature. The chromaticity differences are to be within the specified uncertainties. The expanded uncertainty of the reference colorimeter for tungsten lamp measurements is 4 K (k = 2). This uncertainty is dominated by the uncertainty of the spectral irradiance responsivity calibrations of the channels. If the measurement differences of the test colorimeters increase relative to the measurement results of the reference colorimeters, the spectral responsivity calibrations of the test colorimeters are to be repeated at the SCF to find the reason of the changes.

10. Alternative matrix corrections

Tristimulus meters are fast compared to monochromator based colorimeters. However, they have not been used for solid state light (SSL) source measurements because the measurement uncertainties could be high. The reason of the large uncertainties is that the spectral mismatch of the realized tristimulus channels can be different at certain wavelength intervals compared to the CIE standard color matching functions (CMF). Since the number of the color filter types and also the number of the filter layers that can be used in front of a Si photodiode are limited, the spectral mismatch errors cannot be decreased to the required small values. The spectral mismatch errors can be especially high when narrowband SSL sources are measured. The performed matrix-based color corrections for different light-source distributions show how the matrix elements can be optimized to obtain the smallest errors for special (such as SSL) source distributions [16].

In order to increase the number of the colorimeter channels, one of the second generation colorimeters was extended with an additional (fifth) channel to apply spectral mismatch corrections for certain wavelength intervals of the X_1, X_2, Y, and Z channels where the realized responsivity deviation from the CIE standard color matching functions was significant. A matrix transformation for the A/D converted signals of the five channels was used to correct for any poor spectral match in the realized channels and to perform low-uncertainty color measurement. The correction matrices were designed such that the spectral mismatch errors of the realized functions were minimized relative to the CIE standard CMF functions for several selected test-source distributions such as LEDs.

The spectral responsivity function of the added channel was realized such that the missing or excess (spectral) responsivity components in the realized four channels (where the spectral match is poor) can be corrected for different test-source distributions using a matrix transformation for the signals from the five channels. The selectable test source distributions can be different temperature tungsten lamps, different LEDs, and their mix. Using a high resolution A/D converter, the analog output voltages of the five channels are converted into digital numbers that can be corrected by a software-matrix and then multiplied by the channel calibration factors. When the matrix is used, the color correction factors (the integral ratios) within the calibration factors are changed to unity and the matrix performs the spectral mismatch corrections [7].

The color measurement errors (color differences) with and without matrix corrections were compared using simulations [7]. The simulations included the chromaticity calculation of several source distributions. The real chromaticity values were calculated from the spectral products of monochromator measured (or Planckian) source distributions and the CIE standard 2° color matching functions. The modeled chromaticity values from the calculated output current of the channels (which is equal to the spectral product of the measured or Planckian source distribution and the realized and measured channel spectral responsivities) were compared to the real chromaticity values. Also, the matrix corrected chromaticity values were calculated and compared to the real values. The chromaticity differences were small and similar to each other (average $\Delta(u',v') = 2.8 \times 10^{-4}$) without matrix use (obtained with the detector-based calibration) when Planckian sources were modeled. However, the color differences were about twenty times larger (average $\Delta(u',v') = 5.7 \times 10^{-3}$ when LEDs were measured. When matrix corrections were used with the detector-based calibration, the spectral mismatch corrections could be significantly improved for solid-state light sources including LEDs. The average modeled chromaticity differences (referenced to the real chromaticity values) were more than 20 times smaller with the applied matrix corrections.

11. Conclusions

New generation tristimulus colorimeters with illuminance measuring channels and working standard photometers have been developed at NIST to improve the uncertainty of the illuminance unit (the NIST photometric scale) and also to implement/introduce the first detector-based color

scale. The transfer standard tristimulus meters were designed such that it is the uncertainty of the spectral irradiance responsivity calibrations that determines the photometric and colorimetric scale uncertainties and not the limitations in the performance of the meters themselves. Low illuminance- and color-measurement uncertainties were required for the calibration and measurement of all kinds of light sources. The reference tristimulus meter was calibrated both at the SIRCUS and the SCF facilities. After minimizing the systematic calibration errors at the SCF, the 0.4% difference in the illuminance responsivities obtained at the SIRCUS and the SCF facilities decreased to 0.04%. The uncertainty of the illuminance unit was decreased from 0.39% (k = 2) to 0.2% (k = 2). The working standard tristimulus meters and photometers were calibrated at the SCF. The NIST developed detector-based tristimulus color scale [3] was implemented. The calibrations were based on low-uncertainty spectral responsivity measurements of the colorimeter channels. The working standard tristimulus meters were also calibrated against the reference tristimulus meter in broad-band measurement mode to decrease color measurement uncertainties especially in the blue channels where the uncertainties of the calibration factors were larger. The detector- and source-based color temperature calibrations were compared. The agreement was within 3 K when a tungsten lamp-standard was measured at 2856 K and 3100 K. The detector-based color temperature calibration uncertainty of tungsten lamps decreased to 4 K (k = 2) from the 8 K (k = 2) uncertainty of the presently used NIST source-based scale. One second generation tristimulus meter was extended with a fifth channel to apply software implemented matrix corrections for improving the spectral mismatch errors in special test (such as SSL) source measurements. The matrix produced decrease in the chromaticity differences, as calculated from modeling, was a factor of twenty for color LEDs.

References

[1] Eppeldauer, G.P.; Miller, C.C.; Ohno, Y. In *Proceedings of the 26th Session of the CIE*, Vol. 1, Beijing, China, July 4–11, 2007; D2–99–D2-102; CIE Central Bureau: Vienna, Austria, 2007.

[2] Eppeldauer, G.P.; Miller, C.C.; Larason, T.C.; Ohno, Y. Presented at the CIE Light and Lighting Conference, Budapest, Hungary, May 27–29, 2009.

[3] Eppeldauer, G.P. *J. Res. Natl. Inst. Stand. Technol.* **1998,** *103,* 615–619.

[4] Eppeldauer, G.P.; Miller, C.C.; Larason, T.C.; Ohno, Y. Presented at the CIE Tutorial and Expert Symposium on Spectral and Imaging Methods for Photometry and Radiometry, Bern, Switzerland, August 30–31, 2010.

[5] Cromer, C.L.; Eppeldauer, G.P.; Hardis, J.E.; Larason, T. C.; Ohno, Y.; Parr, A.C. *J. Res. Natl. Inst. Stand. Technol.* **1996,** *101,* 109–132.

[6] Brown, S.W.; Eppeldauer, G.P.; Lykke, K.R. *Appl. Opt.* **2006,** *45,* 8218–8237.

[7] Eppeldauer, G.P.; Kosztyan, Z.; Schanda, J.D.; Schanda, G.; Miller, C.C.; Larason, T.C.; Ohno, Y. Presented at the CIE Light and Lighting Conference, Budapest, Hungary, May 27–29, 2009.

[8] CIE. *The Basis of Physical Photometry.* CIE Central Bureau: Vienna, Austria, 1983.

[9] Eppeldauer, G.P.; Lynch, D.C. *J. Res. Natl. Inst. Stand. Technol.* **2000,** *105,* 813–828.

[10] Larason, T.C.; Eppeldauer, G.P.; Houston, J.M.; Bruce, S. S.; Brown, S.W.; Lykke, K.R. Presented at the NEWRAD Conference at NIST, Gaithersburg, MD, May 20–24, 2002.

[11] Fowler, J.; Litorja, M. *Metrologia* **2003,** *40,* S9–S12.

[12] Eppeldauer, G.P. *J. Metrol. Soc. India* **2009,** *24,* 193–202.

[13] Eppeldauer, G.P.; Miller, C.C.; Ohno, Y. In *Proceedings of CIE Expert Symposium on Advances in Photometry and Colorimetry*; CIE Central Bureau: Vienna, Austria, 2008, pp. 141–146.

[14] Larason, T.C.; Houston, J.M. *Spectroradiometric Detector Measurements: Ultraviolet, Visible, and Near-infrared Detectors for Spectral Power*; NIST Special Publication 250–41; NIST Printing Office, US Department of Commerce, 2008.

[15] Yoon, H.W.; Gibson, C.E.; Barnes, P.Y. *Appl. Opt.* **2002,** *41,* 5879–5890.

[16] Kosztyan, Z.; Eppeldauer, G.P.; Schanda, J.D. *Appl. Opt.* **2010,** *49,* 2288–2301.